

## Potential Use of High Thermal-Conductivity Fuels in Advanced Heavy-Water Moderated Reactors

W. Peiman, I. Pioro, and K. Gabriel<sup>1</sup>

University of Ontario Institute of Technology

Faculty of Energy Systems and Nuclear Science

<sup>1</sup>Faculty of Engineering and Applied Science

2000 Simcoe Street North, Oshawa, Ontario, L1H 7K4, Canada

[wargha.peiman@uoit.ca](mailto:wargha.peiman@uoit.ca), [igor.pioro@uoit.ca](mailto:igor.pioro@uoit.ca), [kamiel.gabriel@uoit.ca](mailto:kamiel.gabriel@uoit.ca)

### Abstract

This paper focuses on the investigation of the potential use of high thermal-conductivity fuels such as uranium dioxide plus silicon carbide (UO<sub>2</sub>-SiC), uranium dioxide plus beryllium oxide (UO<sub>2</sub>-BeO), and uranium dioxide composed of graphite fibers (UO<sub>2</sub>-C) in SuperCritical Water-cooled Reactors (SCWRs), which are considered as advanced heavy-water moderated reactors. The objective of this paper is to evaluate several high thermal-conductivity fuels, namely, UO<sub>2</sub>-SiC, UO<sub>2</sub>-BeO, and UO<sub>2</sub>-C. In order to fulfill the objective of this paper, the fuel centerline temperature and sheath temperature profiles of these fuels have been calculated and compared against the industry accepted limit and the design limit of 1850°C and 850°C for the fuel and the sheath, respectively. The result showed that the fuel centerline temperatures of the examined high thermal conductivity fuels are below the temperature limit of 1850°C under the operating conditions of the SCWR fuel channels with the maximum thermal power when 43-element fuel bundles, which have 42 fuel elements with an outer diameter of 11.5 mm, are used.

### 1. Introduction

The Generation IV International Forum (GIF) has focused on the development of six nuclear-reactor concepts, which pave the road to clean and sustainable energy production. These six nuclear reactor concepts are Gas-cooled Fast Reactor (GFR), Sodium-cooled Fast Reactor (SFR), Lead-cooled Fast Reactor (LFR), Very-High-Temperature Reactor (VHTR), Molten Salt Reactor (MSR), and SuperCritical-Water-cooled Reactor (SCWR) [1]. One common feature of these reactors is that they operate at higher temperatures between 510°C and 1000°C, compared with those of the current water-cooled reactors (e.g., less than 330°C) [1]. The high operating temperatures not only increase the thermal efficiency of the Generation IV Nuclear Power Plants (NPPs), but also it allows for the co-generation of hydrogen.

Among the Generation IV nuclear-reactor concepts, only SCWRs use water as the coolant. Furthermore, thermal-spectrum pressure-tube SCWRs use heavy water as the moderator. Thus, SCWRs are considered as the future of both light-water and heavy-water reactors due to the utilization of both light water and heavy water as the coolant and the moderator, respectively. SCWRs will have high thermal efficiencies within the range of 45 - 48% owing to high reactor-outlet temperatures. A generic SCWR operates at a pressure of 25 MPa with inlet- and outlet-coolant temperatures of 350°C and 625°C [2]. The high outlet temperature and pressure make it possible to use supercritical “steam” turbines, which lead to high thermal efficiencies at coal-fired power plants. Additionally, there is a possibility for co-generation of hydrogen using high-temperature heat from an SCWR during off-peak

hours. For instance, hydrogen production using copper-chlorine cycle requires steam at temperatures as high as 530°C [3, 4], which can be supplied from an SCW nuclear power plant through an intermediate heat exchanger(s).

High operating temperatures of SCWRs leads to high fuel centerline temperatures. Previous studies [5-7] have shown that the fuel centerline temperatures could exceed the industry limit of 1850°C when UO<sub>2</sub> is used at SCWR conditions. Therefore, there is a need for alternative fuels for future use in SCWRs. The objective of this paper is to investigate a possibility of using high thermal-conductivity fuels such as uranium dioxide plus silicon carbide (UO<sub>2</sub>-SiC), uranium dioxide plus beryllium oxide (UO<sub>2</sub>-BeO), and uranium dioxide composed of graphite fibbers (UO<sub>2</sub>-C) in SCWRs. The fuel centerline temperature has been calculated for a pressure channel SCWR in which the core is composed of distributed fuel channels. In the present paper, we have tended to use a conservative analysis approach, which is based on the fuel channels with the maximum thermal power, i.e., +15% above the average channel power, instead of using an average thermal power per channel.

### 1.1 Parameters of a Generic PT SCWR

The core of a generic 1200-MW<sub>el</sub> PT SCWR with single-reheat cycle consists of 300 fuel channels, which are located inside a cylindrical vessel, which is called the Calandria vessel. There are 220 SuperCritical Water (SCW) fuel channels with an average thermal power of 8.5 MW, and 80 Steam Re-Heat (SRH) fuel channels with an average thermal power of 5.5 MW.

The inlet and outlet temperatures of the coolant (e.g. supercritical water) in SCW channels are 350°C and 625°C at a pressure of approximately 25 MPa. The inlet temperature of the coolant (e.g. superheated steam) in the SRH fuel channels is 400°C, and reaches an outlet temperature of 625°C at an operating pressure of 5.7 MPa. There are 12 fuel bundles located in each fuel channel. In this paper, the Variant-20 fuel bundle design has been chosen for the purpose of calculating the fuel centreline and sheath temperatures [9]. This fuel bundle has 42 fuel elements with an outer diameter of 11.5 mm and a central element, which contains burnable neutron-absorber and has an outer diameter of 20 mm. Table 1 lists the operating parameters of a generic PT SCWR [8].

**Table 1: Operating Parameters of Generic PT SCWR [8].**

Parameters	Unit	Generic PT SCWR	
Electric Power	MW	1143-1220	
Thermal Power	MW	2540	
Thermal Efficiency	%	45-48%	
Coolant/ Moderator	-	H <sub>2</sub> O/ D <sub>2</sub> O	
Pressure of SCW at Inlet/Outlet	MPa	25.8	25
Pressure of SHS at Inlet/Outlet	MPa	6.1	5.7
$T_{in} / T_{out}$ Coolant (supercritical water)	°C	350	625
$T_{in} / T_{out}$ Coolant (superheated steam)	°C	400	625
Mass Flow Rate per SCW/SRH Channel	kg/s	4.4	9.8
Thermal Power per SCW/SRH Channel	MW	8.5	5.5
# of SCW/SRH Channels	-	220	80
Fuel Bundle	-	Variant-20 <sup>[9]</sup>	

In a single-reheat cycle, the supercritical “steam”, coming out of the SCW fuel channels, expands through a high-pressure turbine. Then, the steam is sent back to the SRH channels, where the temperature of the steam is raised to superheated conditions. Next, the superheated steam expands through the intermediate-pressure turbine. Finally, the steam is transferred to the low-pressure turbines, where the steam is exhausted to the condenser [10].

## 1.2 Fuel Channel Description and Parameters

The Atomic Energy of Canada Limited (AECL) has developed several fuel channel designs for its SCWR concept. One of these designs is the High Efficiency Channel (HEC). The HEC design is a direct-flow fuel channel concept, which consists of 12 fuel bundles, a perforated liner tube, a ceramic insulator, and a pressure tube. In order to minimize the heat losses from the coolant to the moderator a porous ceramic insulator, which is made of Yttria Stabilized Zirconia (YSZ), is placed between the “hot” coolant and “cold” PT. In addition to minimizing the heat losses from the coolant, the ceramic insulator reduces the operating temperature of PT. This allows for the use of currently available materials such as Zr-2.5% Nb, which have low absorption cross sections for thermal neutrons [11]. The liner is a perforated tube made of stainless steel. The ultimate purpose of the liner is to protect the ceramic insulator from being damaged during operation and refuelling due to stresses introduced by the fuel bundles and from erosion by the coolant flow. Figure 1 shows a 3-D view of HEC.

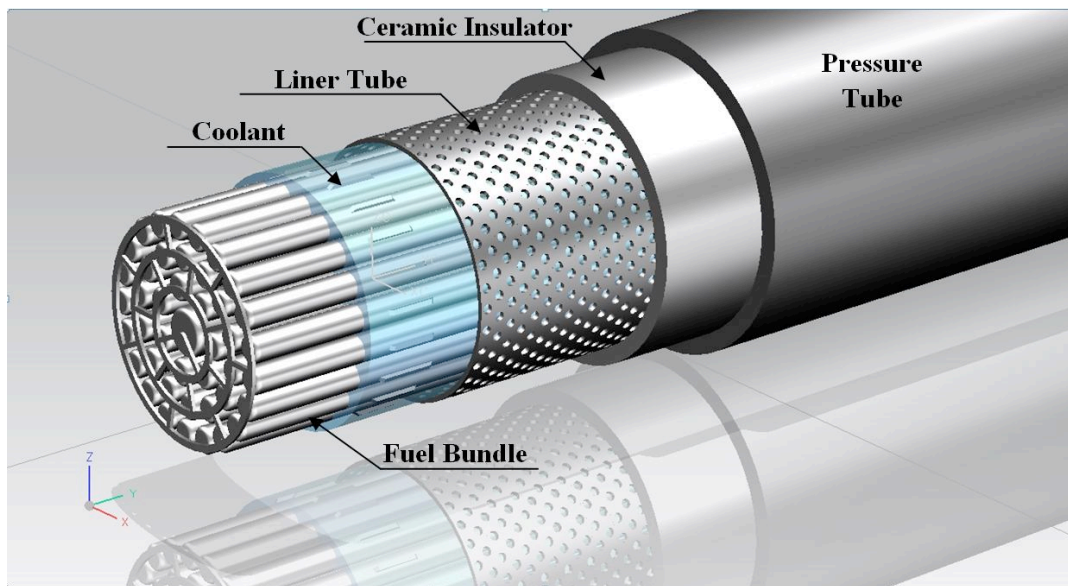


Figure 1: 3-D View of High Efficiency Channel (based on [11]).

## 2. Alternative Fuels

A potential fuel must have a high melting point, high thermal-conductivity, good irradiation, and mechanical stability [11] due to high operating temperatures of SCWRs. These requirements eliminate various nuclear fuels categorized under metallic fuels because of their low melting point, high irradiation induced creep, and high irradiation swelling [11]. On the other hand, ceramic fuels have superior properties, which make these fuels suitable candidates for SCWR.

In terms of thermophysical properties of a fuel, melting point and thermal conductivity are the most important properties. The thermal conductivity of the fuel governs the rate of heat transfer removal

from the fuel under specific conditions (e.g., mass flow rate, heat flux, and fuel bundle geometry).  $\text{UO}_2$  has been used as the fuel of choice in most commercial nuclear reactors. As shown in Fig. 2, the thermal conductivity of  $\text{UO}_2$  is between 2 and 3 W/m K within the operating temperature range of SCWRs. On the other hand, high thermal-conductivity fuels such as UN, UC, and  $\text{UC}_2$  have significantly higher thermal conductivities compared to that of  $\text{UO}_2$ . High thermal conductivities result in lower fuel centerline temperatures and limit the release of gaseous fission products [12]. Thus, under the same operating conditions, the fuel centerline temperature of the high thermal-conductivity fuels should be lower than that of the  $\text{UO}_2$  fuel.

Currently, there is a high interest in improving the thermal conductivity of low thermal-conductivity fuels such as  $\text{UO}_2$ . The increase in the thermal conductivity of  $\text{UO}_2$  can be performed either by adding a continuous solid phase or long, thin fibers of a high thermal-conductivity material [12, 13]. A high thermal-conductivity material must have a low thermal-neutron absorption cross-section, assuming that the fuel will be used in a thermal-spectrum nuclear reactor [12]. Additionally, it must have a high melting point and be chemically compatible with the fuel, the cladding, and the coolant. The need to meet the aforementioned requirements narrows the potential materials to silicon carbide (SiC), beryllium oxide (BeO), and graphite (C). The following sections provide some information about the  $\text{UO}_2$  fuel composed of the aforementioned high thermal-conductivity materials.

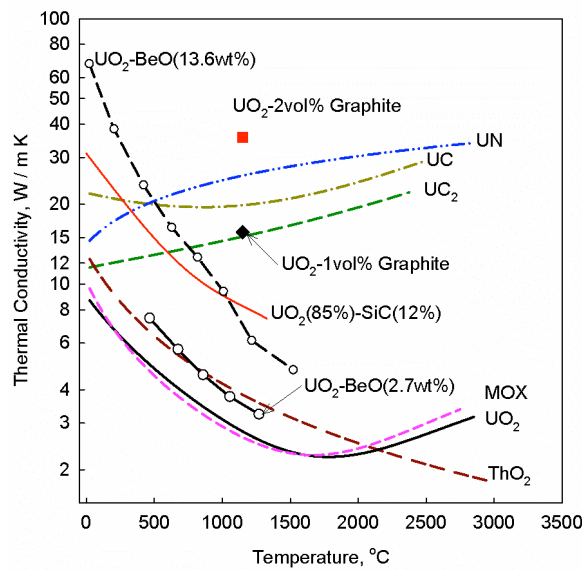


**Figure 2: Thermal Conductivities of  $\text{UO}_2$ , MOX,  $\text{ThO}_2$ , UN, UC,  $\text{UC}_2$ ,  $\text{UO}_2\text{-SiC}$ ,  $\text{UO}_2\text{-BeO}$ , and  $\text{UO}_2\text{-C}$  Fuels as a Function of Temperature [12-20].**

## 2.1 Uranium Dioxide plus Silicon Carbide ( $\text{UO}_2\text{-SiC}$ )

The thermal conductivity of the  $\text{UO}_2$  fuel can be improved by incorporating silicon carbide (SiC) into the matrix of the fuel. SiC has a high melting point approximately at  $2800^\circ\text{C}$ , high thermal-conductivity (78 W/mK at  $727^\circ\text{C}$ ), high corrosion resistance even at high temperatures, low thermal neutron absorption cross-section, and dimensional stability [20]. Therefore, when used with  $\text{UO}_2$ , SiC can address the problem of poor thermal-conductivity of the  $\text{UO}_2$  fuel.

Calculation of the thermal conductivity of the UO<sub>2</sub> plus SiC fuel falls under the theories of composites. Generally, theories contemplating the thermal conductivity of composites are classified into two categories. One category assumes that inclusions are randomly distributed in a homogeneous mixture. The Effective Thermal Conductivities (ETCs) of the composites, based on the aforementioned principle, are formulated by Maxwell. The other category, which is based on the work performed by Rayleigh, assumes that particles are distributed in a regular manner within the matrix.

Khan et al. have provided the thermal conductivity of the UO<sub>2</sub>-SiC fuel as a function of temperature and weight percent of SiC. They assumed that the thin coat of SiC covered UO<sub>2</sub> particles and determined the thermal conductivity of the composite fuel based on the Rayleigh equation shown as Eq. (1) [20].

$$k_{eff\ R(\psi)} = k_{SiC} \cdot \left[ 1 + 3 \frac{\psi}{\left[ \frac{k_{UO_2} + 2k_{SiC}}{3k_{UO_2} - k_{SiC}} \right]^{-\psi + 1.569} \left[ \frac{k_{UO_2} - k_{SiC}}{3k_{UO_2} - 4k_{SiC}} \right]^{-\psi^{10/3}}} \right] \quad (1)$$

In the present study, the UO<sub>2</sub>-SiC fuel with 12wt% SiC has been examined and its thermal conductivity has been calculated using Eq. (2) [20].

$$k_{eff} = -9.59 \times 10^{-9} T^3 + 4.29 \times 10^{-5} T^2 - 6.87 \times 10^{-2} T + 4.68 \times 10^{+1} \quad (2)$$

## 2.2 Uranium Dioxide plus Graphite Fibbers (UO<sub>2</sub>-C)

Hollenbach and Ott have studied the effects of the addition of graphite fibbers on thermal conductivity of the UO<sub>2</sub> fuel. Theoretically, the thermal conductivity of graphite varies along different crystallographic planes. For instance, the thermal conductivity of perfect graphite along basal planes is more than 2000 W/m K [12]. On the other hand, it is less than 10 W/m K in the direction perpendicular to the basal planes. Hollenbach and Ott have performed computer analyses in order to determine the effectiveness of adding long, thin fibbers of high thermal-conductivity materials to low thermal-conductivity materials to determine ETC. In their studies, the high thermal-conductivity material had a thermal conductivity of 2000 W/m K along the axis, and a thermal conductivity of 10 W/m K radially, similar to perfect graphite. The low thermal-conductivity material had properties similar to UO<sub>2</sub> (e.g., with 95% TD at ~1100°C) with a thermal conductivity of 3 W/m K.

Hollenbach and Ott have examined the ETC of the composite for various volume percentages of the high thermal-conductivity material, varying from 0 to 3%. Figure 3 shows that the addition of just one volume percent (1 vol %) of high thermal-conductivity material increases the ETC of the composite approximately by a factor of 5. Moreover, if the amount of the high thermal-conductivity material increases to 2 vol %, the ETC of the composite reaches the range of the high thermal-conductivity fuels, such as UN and UC.

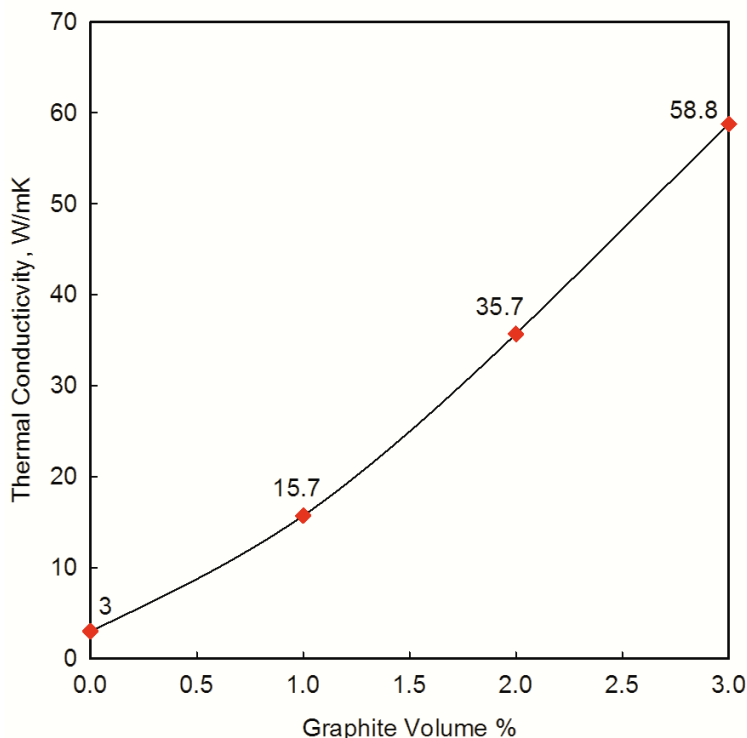


**Figure 3: Thermal Conductivity of  $\text{UO}_2\text{-C}$  as a Function of Volume Percent of Graphite Fibbers [12].**

In this study, the fuel centerline temperature has been calculated at SCWR conditions for the  $\text{UO}_2$  fuel composed of 1 vol % graphite fibbers. Since the thermal conductivity as a function of temperature was not available, the fuel centerline temperature calculation has been conducted based on a constant thermal conductivity shown in Fig. 3.

### 2.3 Uranium Dioxide plus Beryllium Oxide ( $\text{UO}_2\text{-BeO}$ )

Beryllium oxide ( $\text{BeO}$ ) is a metallic oxide with a very high thermal-conductivity.  $\text{BeO}$  is chemically compatible with  $\text{UO}_2$ , most sheath materials including zirconium alloys, and water. In addition to its chemical compatibility with  $\text{UO}_2$ ,  $\text{BeO}$  is insoluble in  $\text{UO}_2$  at temperatures up to  $2160^\circ\text{C}$ . As a result,  $\text{BeO}$  remains as a continuous second solid phase in the  $\text{UO}_2$  fuel matrix while being in good contact with  $\text{UO}_2$  molecules at the grain boundaries.  $\text{BeO}$  has desirable thermochemical and neutronics properties, which have resulted in the use of  $\text{BeO}$  in aerospace, electrical and nuclear applications. For example,  $\text{BeO}$  has been used as the moderator and the reflector in some nuclear reactors. However, the major concern with beryllium is its toxicity. But, the requirements for safe handling of  $\text{BeO}$  are similar to those of  $\text{UO}_2$ . Therefore, the toxicity of  $\text{BeO}$  is not a limiting factor in the use of this material with  $\text{UO}_2$  [13].

Similar to other high thermal-conductivity fuels, the thermal conductivity of  $\text{UO}_2$  can be increased by introducing a continuous phase of  $\text{BeO}$  at the grain boundaries. The effects of the presence of such second solid phase on the thermal conductivity of  $\text{UO}_2$  is significant such that only 10 vol% of  $\text{BeO}$  would improve the thermal conductivity of the composite fuel by 50% compared to that of  $\text{UO}_2$  with

95% TD. Figure 4 shows the thermal conductivity of  $\text{UO}_2\text{-BeO}$  as a function of temperature for 0.9 wt%, 2.7 wt%, 10.2 wt%, 20.4 wt% of BeO [13, 21-23]. For the purpose of this study, a  $\text{UO}_2\text{-BeO}$  fuel with 13.6 wt% of BeO has been examined.

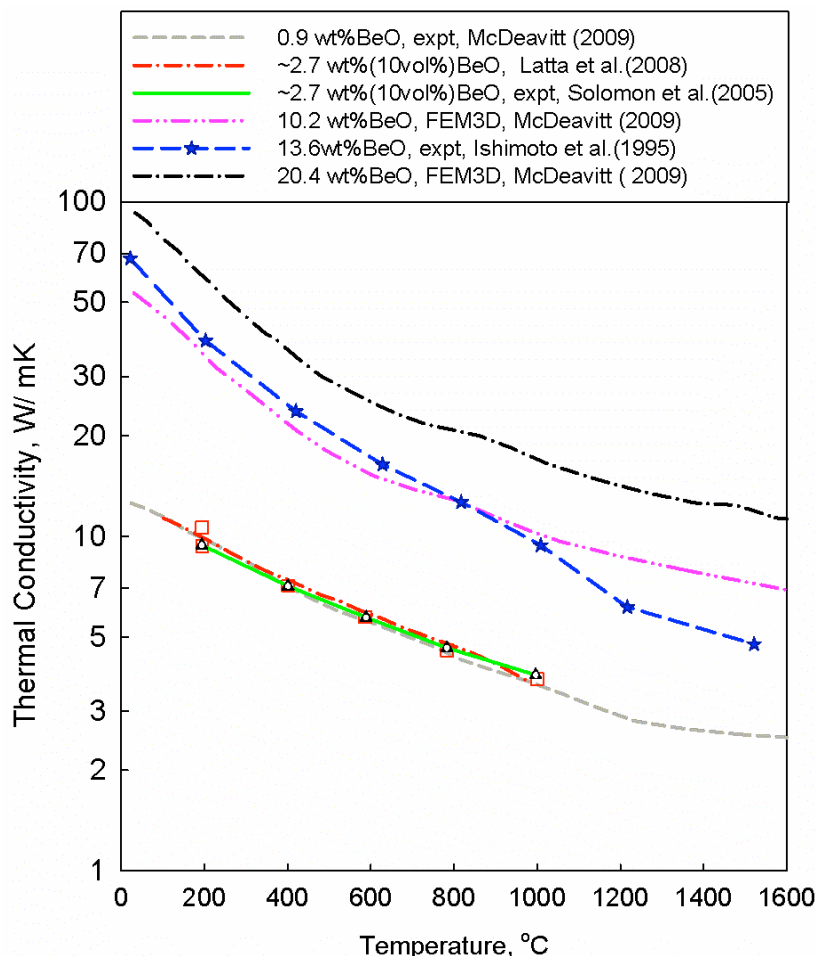


Figure 4: Thermal Conductivity of  $\text{UO}_2\text{-BeO}$  as a Function of Temperature [13, 21-23].

### 3. Calculation of Fuel Centerline Temperature

In order to calculate the fuel centerline temperature, steady-state one-dimensional heat-transfer analysis was conducted. The MATLAB and NIST REFPROP software were used for programming and retrieving thermophysical properties of a light-water coolant, respectively. First, the heated length of the fuel channel was divided into small segments of one-millimeter lengths. Second, a temperature profile of the coolant was calculated. Third, sheath-outer and inner surface temperatures were calculated. Fourth, the heat transfer through the gap between the sheath and the fuel was determined and used to calculate the outer surface temperature of the fuel. Finally, the temperature of the fuel in the radial and axial directions was calculated. It should be noted that the radius of the fuel pellet was divided into 20 segments. The results have been presented for a fuel-sheath gap width of  $20\ \mu\text{m}$ . The following equations were used, in sequence, to determine the coolant, sheath [24], and fuel centerline temperature profiles.

Equation (3) was used to calculate the enthalpy profile of the coolant. Then, NIST REFPROP was used to determine the corresponding temperature profile of the coolant based on calculated enthalpies. In other words, for each point along the heated length of the fuel channel enthalpy was calculated.

Next, the calculated enthalpy and pressure of the coolant were entered into the NIST REFPROP software as two independent variables to calculate the corresponding temperature of the coolant.

Since the temperature profile of the coolant was calculated based on Eq. (3), the outer surface temperature of the sheath was calculated using Eq. (4). The latter equation requires the calculation of the Heat Transfer Coefficient (HTC) between the sheath-wall and the coolant. HTC was calculated using the Mokry et al. correlation [25] shown as Eq. (5). Then, the inner sheath temperature was calculated based on conduction through the sheath using Eq. (6).

$$H_{i+1} = H_i + \frac{P \cdot q_x}{\dot{m}} \cdot \Delta x \quad (3)$$

$$T_{sheath} = \frac{q}{h} + T_{coolant} \quad (4)$$

$$Nu_b = 0.0061 Re_b^{0.904} Pr_b^{0.684} \left( \frac{\rho_w}{\rho_b} \right)^{0.564} \quad (5)$$

$$T_{sheath,i} = T_{sheath,o} + Q \cdot \frac{\ln(r_o/r_i)}{2\pi L k} \quad (6)$$

Zahlan et al. [26] have compared sixteen correlations including the Mokry correlation. The result of their comparison showed that the Mokry et al. correlation resulted in the lowest Root-Mean-Square (RMS) error within the supercritical region compared to other correlations. The experimental data, on which the Mokry et al. correlation was developed, were obtained within conditions similar to those of proposed SCWR concepts. The experimental dataset was obtained for supercritical water flowing upward in a 4-m-long vertical bare tube. The data was collected at a pressure of approximately 24 MPa for several combinations of wall and bulk fluid temperatures which were below, at, or above the pseudocritical temperature. The mass flux ranged from 200-1500 kg/m<sup>2</sup>s; coolant inlet temperature varied from 320°C to 350°C, for heat flux up to 1250 kW/m<sup>2</sup> [25].

In Equation (3),  $q$  is the heat flux value, which varies along the axial direction of the fuel channel. In this paper, several Axial Heat Flux Profiles (AHFPs) have been used to calculate the fuel centerline temperature at the channels with the maximum thermal power. The maximum channel power was assumed to be 15% (10% variation in thermal power and 5% uncertainty) above the average thermal power. Consequently, heat flux profiles have been calculated based on a maximum thermal power per channel of 9.8 MW<sub>th</sub>. These AHFPs, which include cosine, upstream-skewed cosine, downstream-skewed cosine, and uniform, listed in Reference [9]. It should be noted that upstream-skewed AHFP was determined as the mirror image of the downstream-skewed AHFP. Figure 5 shows the power ratios based on which AHFPs have been determined. The power ratio has been defined as the ratio of the local heat flux to the average heat flux. A 43-element bundle (i.e. Variant-20) was used in order to determine the average heat flux.

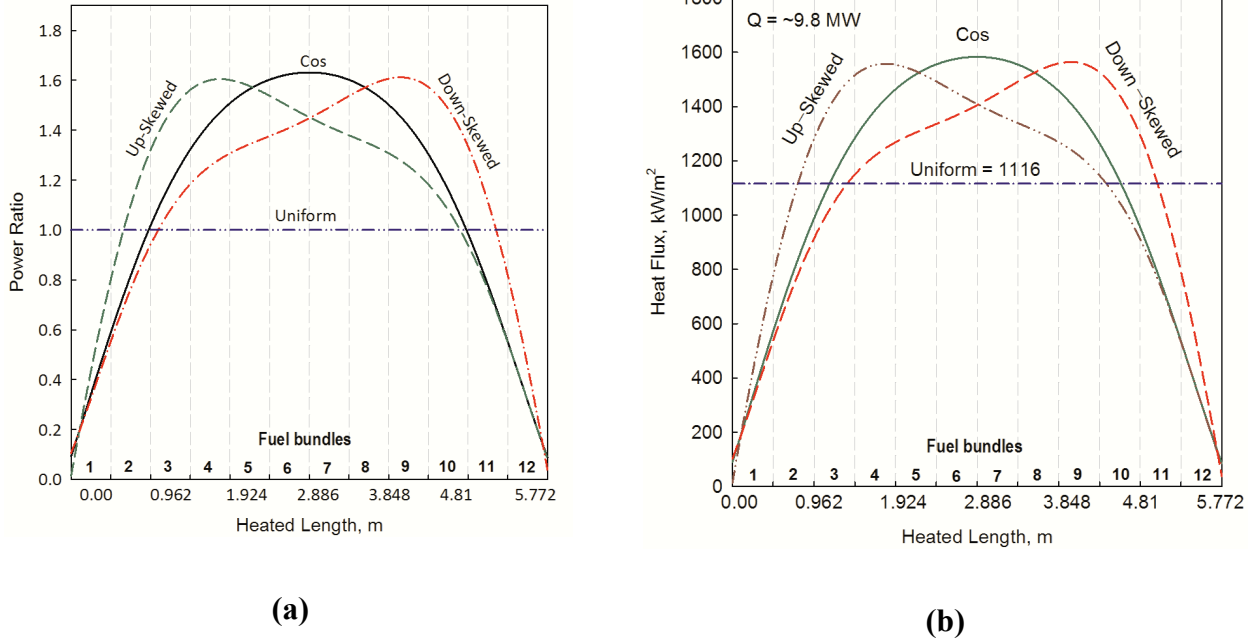


**Figure 5: (a) Power Ratios [24], and (b) Heat Fluxes for Uniform, Cosine, Upstream-Skewed, and Downstream-Skewed Profiles for SCW Fuel Channels with Maximum Thermal Power.**

In the present study, the modified Ross and Stoute model has been used in order to determine the gap conductance effects on the fuel centerline temperature. In this model, the total heat transfer through the gap is calculated as the sum of heat transfer through the gas, heat transfer due to contacts between the fuel and the sheath, and the radiative heat transfer as represented in Eq. (7).

$$h_{total} = h_g + h_c + h_r \quad (7)$$

The heat transfer through the gas in the fuel-sheath gap is by conduction because the gap width is very small. This small gap width does not allow for the development of natural convection through the gap. The heat transfer rate through the gas is calculated using Eq. (8).

$$h_g = \frac{k_g}{1.5(R_1 + R_2) + t_g + g} \quad (8)$$

The fuel-sheath gap is very small, in the range between 0.0 and 125  $\mu\text{m}$  [27]. CANada DUterium (CANDU) reactors use collapsible sheath, which leads to small fuel-sheath gaps approximately 20  $\mu\text{m}$  [28]. Moreover, Hu and Wilson [29] have reported a fuel-sheath gap width of 36  $\mu\text{m}$  for a proposed PV SCWR. In this paper, the fuel centerline temperature has been calculated for 20- $\mu\text{m}$  fuel-sheath gap. In Equation (8),  $g$  is the temperature jump distance, which is calculated using Eq. (9) [30].

$$\frac{1}{g} = \sum_i \left[ \frac{y_i}{g_{o,i}} \right] \left( \frac{T_g}{273.15} \right)^{s+1/2} \left( \frac{0.101}{P_g} \right) \quad (9)$$

In reality, the fuel pellets become in contact with sheath creating contact points. These contact points are formed due to thermal expansion and volumetric swelling of fuel pellets. As a result, heat is

transferred through these contact points. The conductive heat transfer rate at the contact points are calculated using Eq. (10) [31]. In Eq. (10),  $A$  and  $n$  are equal to 10 and 0.5.

$$h_c = A \frac{2k_f k_{sheath}}{(k_f + k_{sheath}) \left[ \frac{R_f^2 + R_{sheath}^2}{2} \right]^{1/2}} \cdot \left( \frac{P_a}{HD} \right)^n \quad (10)$$

The last term in Eq. (7) is the radiative heat transfer coefficient through the gap, which is calculated using Eq. (11) [31]. It should be noted that the contribution of this heat transfer mode is negligible under normal operating conditions. However, the radiative heat transfer is significant in accident scenarios. Nevertheless, the radiative heat transfer through the fuel-sheath gap has been taken into account in this paper.

$$h_r = \frac{\sigma \varepsilon_f \varepsilon_{sheath}}{\varepsilon_f + \varepsilon_{sheath} - \varepsilon_f \varepsilon_{sheath}} \cdot \frac{(T_{f,o}^4 - T_{sheath,i}^4)}{(T_{f,o} - T_{sheath,i})} \quad (11)$$

Knowing the total heat transfer coefficient across the fuel-sheath gap, the outer surface temperature of the fuel was calculated. Then, Eq. (12) was used in order to calculate the fuel centerline temperature profile. It should be mentioned that the radius of the fuel was divided into 20 segments in order to increase the accuracy of the calculations.

$$T_{r,i+1} = \frac{Q_{gen}(r_i^2 - r_{i+1}^2)}{4 \cdot k_{avg}} + T_{r,i} \quad (12)$$

#### 4. Results

The fuel centerline temperature was calculated at SCW channel conditions. A steady-state one-dimensional heat transfer analysis was conducted with fuel channel specifications as follows: a mass flow rate of 4.4 kg/s, a constant pressure of 25 MPa, a coolant inlet temperature of 350°C, a thermal power per channel of 9.8 MW<sub>th</sub>. The heat flux profiles were calculated based on a 43-element fuel bundle known as the Variant-20 fuel bundle. Each of the 42 fuel elements of the Variant-20 fuel bundle has an outer diameter of 11.5 mm while the thickness of the sheath has been determined to be 0.47 mm. Further, it was assumed that the width of the fuel-sheath gaps is 20 μm. Therefore, the outer diameter of the fuel pellets was 10.52 mm. Inconel-600 was chosen as the material of the sheath.

The examined fuels were UO<sub>2</sub>, UO<sub>2</sub>-SiC, UO<sub>2</sub>-BeO, and UO<sub>2</sub>-C with 95% TD. For each fuel, the fuel centerline temperature was analysed for uniform, cosine, upstream-skewed cosine and downstream-skewed cosine AHFPs, which were calculated based on the maximum thermal power per channel of 9.8 MW<sub>th</sub>. Figure 6 shows the coolant, sheath, and fuel centerline temperature profiles along the heated length of the fuel channel for UO<sub>2</sub>, UO<sub>2</sub>-SiC, UO<sub>2</sub>-BeO, and UO<sub>2</sub>-C fuels. Since the maximum fuel centerline temperatures were reached when the downstream-skewed cosine AHFP was applied only the results corresponding to the downstream-skewed cosine AHFP have been presented in Fig. 6.

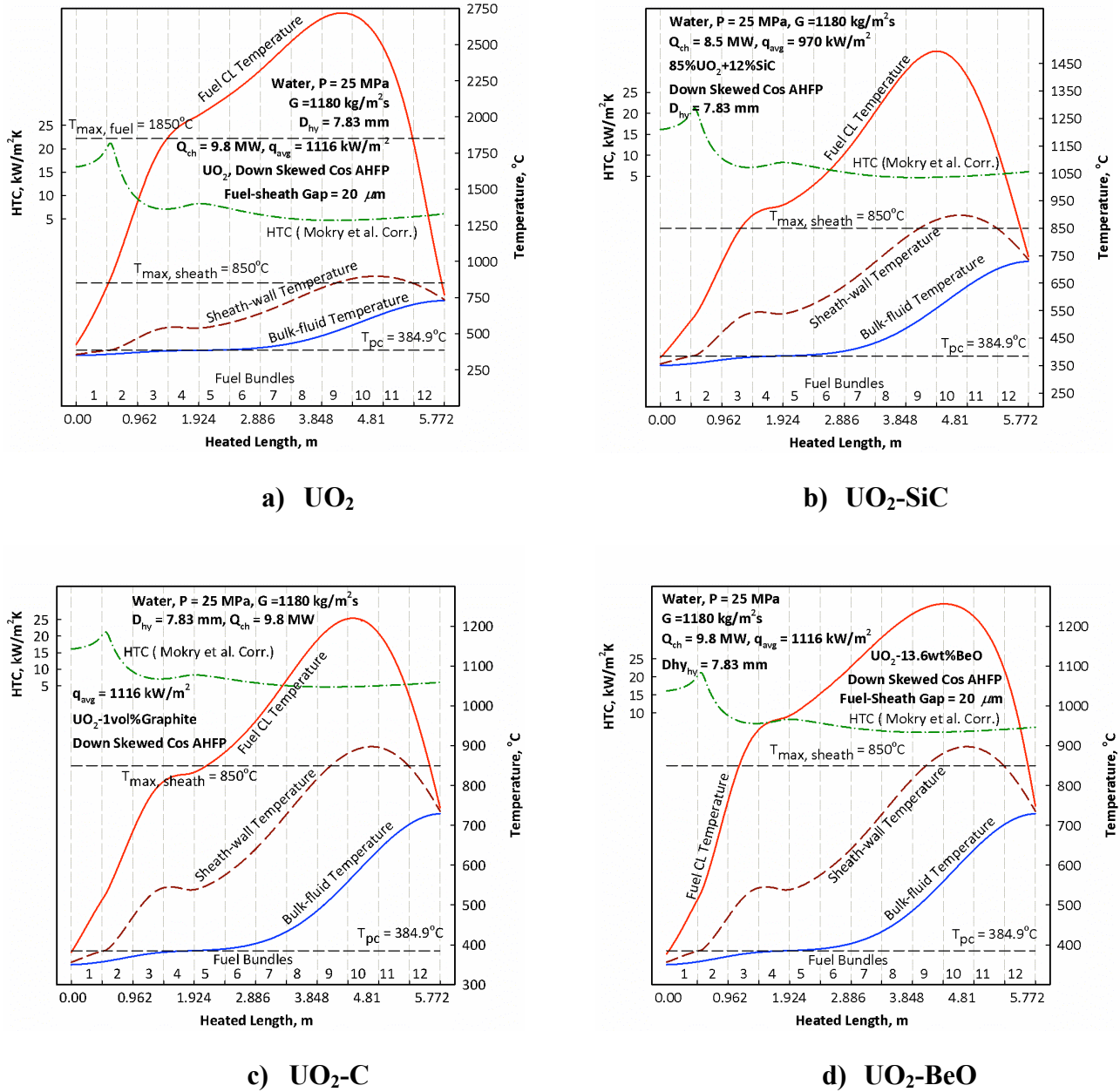


**Figure 6: Bulk-Fluid Temperature, Sheath Temperature, Fuel Centerline Temperature and HTC profiles for  $UO_2$ ,  $UO_2\text{-SiC}$ ,  $UO_2\text{-BeO}$ , and  $UO_2\text{-C}$  Fuels at Downstream-Skewed AHFP and Maximum Channel Power.**

In regards to the sheath temperature, for all the examined fuels, the maximum sheath temperature exceeds the design temperature limit of  $850^\circ\text{C}$  at the downstream-skewed cosine AHFP. In order to meet the design requirement on the sheath temperature, either a new fuel bundles should be designed or the operating conditions of the fuel channels with the maximum thermal power should be modified. A new fuel bundle should have fuel elements with smaller diameters, but the number of fuel elements must be increased to compensate for the reduced volume of the fuel contained in the fuel bundle. In regards to the operating conditions of the fuel channel, the mass flux in fuel channels with the maximum thermal power must be increased. This increase in the mass flux reduces the sheath and the

fuel centerline temperatures while allows the coolant to reach the desirable outlet temperature of 625°C. In fuel channels with the maximum thermal power, the outlet temperature of the coolant exceeds the design outlet temperature of 625°C due to higher heat flux values.

For the UO<sub>2</sub> fuel, the maximum fuel centreline temperature is 2730°C, which exceeds the industry accepted limit of 1850°C. On the other hand, the maximum fuel centreline temperatures of UO<sub>2</sub>-SiC, UO<sub>2</sub>-BeO, and UO<sub>2</sub>-C were 1495°C, 1255°C, and 1220°C, respectively. Therefore, the results indicate that the fuel centreline temperatures of high thermal-conductivity fuels are significantly lower than the temperature limit of 1850°C. This temperature limits has been applied to the examined high thermal-conductivity fuels because firstly, these fuels mostly consist of UO<sub>2</sub>, secondly, the melting points of the added high thermal-conductivity materials (i.e. SiC, BeO, and C) are comparable to that of UO<sub>2</sub>. Therefore, it is reasonable to apply the industry accepted limit of 1850°C to the examined high thermal-conductivity fuels as a basis for comparison.

## 5. Conclusions

The possibility of using several high thermal-conductivity fuels enclosed in a 43-element fuel bundle (i.e. Variant-20) at conditions of an advanced heavy-water moderated nuclear reactor, namely, SCWR was investigated. The fuel centerline temperature profile for the UO<sub>2</sub>, UO<sub>2</sub>-SiC, UO<sub>2</sub>-BeO, and UO<sub>2</sub>-C fuels was calculated as well as the sheath temperature of the Variant-20 fuel bundles along the heated length of the fuel channel. These fuels were examined at the operating conditions of the supercritical water fuel channels with a maximum thermal power per channel of 9.8 MW<sub>th</sub>. The results showed that under the downstream-skewed axial heat flux profile the sheath temperature exceeds the design temperature limit of 850°C when the Variant-20 fuel bundle is used. Therefore, either a new fuel bundle should be designed or the operating conditions of the fuel channel should be modified in order to comply with the design temperature limit of the sheath.

In regards to the fuel centerline temperature, the maximum fuel centreline temperature exceeds the industry limit of 1850°C for UO<sub>2</sub>. The results conclude that if the use of a low thermal-conductivity fuel (e.g., UO<sub>2</sub> or ThO<sub>2</sub>) is considered as an option, a new fuel bundle must be designed. On the other hand, the fuel centreline temperature was below the temperature limit when the UO<sub>2</sub>-SiC, UO<sub>2</sub>-BeO, and UO<sub>2</sub>-C fuels were examined. Thus, the result of the fuel centerline temperature calculation supports the potential use of high thermal-conductivity fuels in SCWRs. Among these examined composite fuels, UO<sub>2</sub>-BeO has better chemical, irradiation, and thermodynamic properties, which make this fuel a potential candidate. However, further study is required in order to ensure the suitability of this fuel under the SCWR conditions.

## 6. Acknowledgements

Financial supports from the NSERC/NRCan/AECL Generation IV Energy Technologies Program and NSERC Discovery Grant are gratefully acknowledged.

## 7. Nomenclature

$A$	cross-sectional area, m <sup>2</sup>
$A_{fl}$	flow area, m <sup>2</sup>

$c_p$	specific heat at constant pressure, J/kg K
$\bar{c}_p$	average specific heat, $(\frac{H_w - H_b}{T_w - T_b})$ , J/kg K
$D$	diameter, m
$D_{hy}$	hydraulic diameter, m
$E$	Young's modulus, MPa
$G$	mass flux, $(m/A_{fl})$ , kg/m <sup>2</sup> s
$H$	enthalpy, J/kg
$h$	heat transfer coefficient, W/m <sup>2</sup> K
$k$	thermal conductivity, W/m K
$L$	length, m
$m$	mass flow rate, kg/s
$P$	pressure, Pa
$P$	percent porosity
$p$	heated perimeter, m
$Q$	heat transfer rate, W
$q$	heat flux, W/m <sup>2</sup>
$Q_{gen}$	volumetric heat generation, W/m <sup>3</sup>
$T$	temperature, K

### Greek symbols

$\alpha$	thermal diffusivity, $(k/\rho C_p)$ , m <sup>2</sup> /s
$\mu$	dynamic viscosity, kg/m s
$\nu$	kinematic viscosity, m <sup>2</sup> /s
$\rho$	density, kg/m <sup>3</sup>

### Non-dimensional numbers

$\mathbf{Nu}_D$	Nusselt number, $\mathbf{Nu}_D = h \cdot D/k$
$\mathbf{Pr}$	Prandtl Number, $\mathbf{Pr} = \mu \cdot c_p/k$
$\bar{\mathbf{Pr}}$	average Prandtl Number, $\bar{\mathbf{Pr}} = \mu \cdot \bar{c}_p/k$
$\mathbf{Re}_D$	Reynolds number, $\mathbf{Re}_D = G \cdot \frac{D_{hy}}{\mu}$

### Subscripts

atm	atmospheric
b	properties calculated at bulk fluid temperature
c	contact
cond	conduction
conv	convection
g	gas
i	inner
m	melting
o	outer

pc	pseudocritical point
r	radiative
vol	volume
w	properties calculated at wall temperature

## Abbreviations

AECL	Atomic Energy of Canada Limited
AGR	Advanced Gas-cooled Reactor
AHFP	Axial Heat Flux Profile
CANDU	CANada Deuterium Uranium
ETC	Effective Thermal Conductivity
GFR	Gas-cooled Fast Reactor
GIF	Generation IV International Forum
HTC	Heat Transfer Coefficient
HTR	High Temperature Reactor
IAEA	International Atomic Energy Agency
LFR	Lead-cooled Fast Reactor
LWR	Light Water Reactor
MSR	Molten Salt Reactor
NIST	National Institute of Standards and Technology (USA)
NPP	Nuclear Power Plant
PCh	Pressure Channel
PT	Pressure Tube
PV	Pressure Vessel
SCW	SuperCritical Water
SCWR	SuperCritical Water-cooled Reactor
SFR	Sodium-cooled Fast Reactor
SHR	Steam Re-Heat
TD	Theoretical Density
UC	Uranium Carbide
UC <sub>2</sub>	Uranium dicarbide
UN	Uranium Nitride
UO <sub>2</sub>	Uranium dioxide
UO <sub>2</sub> -BeO	Uranium dioxide plus beryllium oxide
UO <sub>2</sub> -C	Uranium dioxide composed of graphite fibbers
UO <sub>2</sub> -SiC	Uranium dioxide plus silicon carbide
VHTR	Very-High-Temperature Reactor

## 8. References

- [1] U.S. DOE Nuclear Energy Research Advisory Committee, "A Technology Roadmap for Generation IV Nuclear Energy Systems", Retrieved 2010 July 12, from the Generation IV International Forum: [http://www.ne.doe.gov/genIV/documents/gen\\_iv\\_roadmap.pdf](http://www.ne.doe.gov/genIV/documents/gen_iv_roadmap.pdf).
- [2] I. L. Pioro, and R. B. Duffey,(2007). "Heat Transfer and Hydraulic Resistance at Supercritical Pressure in Power-Engineering Applications". ASME, New York.
- [3] G., Naterer, S., Suppiah, M., Lewis, (2009). "Recent Canadian Advances in Nuclear-Based Hydrogen Production and the Thermochemical Cu-Cl Cycle", International Journal of Hydrogen Energy (IJHE), Vol. 34, pp. 2901-2917.

- [4] G.F. Naterer, S. Suppiah, L. Stolberg et al., (2010). "Canada's Program on Nuclear Hydrogen Production and the Thermochemical Cu-Cl Cycle", International Journal of Hydrogen Energy (IJHE), Vol. 35, pp. 10905-10926.
- [5] L. Grande, S. Mikhael, B. Villamere, A. Rodriguez-Prado, L. Allison, W. Peiman and I. Pioro, (2010) "Thermal Aspects of Using Uranium Nitride in Supercritical Water-Cooled Nuclear Reactors", Proceedings of the 18<sup>th</sup> International Conference On Nuclear Engineering (ICONE-18), Xi'an, China, May 17-21.
- [6] I. Pioro, S. Mokry, W. Peiman, L. Grande and Eu. Saltanov, (2010). "Supercritical Water-Cooled Nuclear Reactors: NPP Layouts and Thermal Design Options of Pressure Channels", Proceedings of the 17<sup>th</sup> Pacific Basin Nuclear Conference (PBNC-2010), Cancun, Mexico, October 24-30.
- [7] B. Villamere, L. Allison, L. Grande, S. Mikhael, A. Rodriguez-Prado and I. Pioro, (2009). "Thermal aspects for uranium carbide and uranium dicarbide fuels in supercritical water-cooled nuclear reactors", Proceedings of the 17<sup>th</sup> International Conference On Nuclear Engineering, Brussels, Belgium, July 12-16.
- [8] M. Naidin, I. Pioro, R. Duffey, U. Zirn and S. Mokry, (2009). "SCW NPPs: Layouts and Thermodynamic Cycles Options", Proceeding of International Conference "Nuclear Energy for New Europe", Bled, Slovenia, Sep. 14-17.
- [9] L. K. H. Leung, (2009). "Effect of CANDU Bundle-Geometry Variation on Dryout Power", Proceedings of the 16<sup>th</sup> International Conference On Nuclear Engineering, Orlando, USA, May 11-15.
- [10] I. Pioro, S. Mokry, W. Peiman, L. Grande and Eu. Saltanov, (2009). "Supercritical Water-Cooled Nuclear Reactors: NPP Layouts and Thermal Design Options of Pressure Channels", Proceedings of the 17<sup>th</sup> Pacific Basin Nuclear Conference (PBNC-2010), Cancun, Mexico, October 24-30.
- [11] C. K. Chow and H.F. Khartabil, (2008). "Conceptual Fuel Channel Designs for CANDU-SCWR", Journal of Nuclear Engineering and Technology, Vol. 40, 2, pp. 1-8.
- [12] D. F. Hollenbach and L. J. Ott, (2010). "Improving the Thermal Conductivity of UO<sub>2</sub> Fuel with the Addition of Graphite Fibers", Transactions of the American Nuclear Society and Embedded Topical Meeting "Nuclear Fuels and Structural Materials for the Next Generation Nuclear Reactors", San Diego, California, USA, June 13-17.
- [13] Solomon, A. A., Revankar, S., & McCoy, J. K. (2005). *Enhanced Thermal Conductivity Oxide Fuels*. US Department of Energy, Project No. 02-180.
- [14] IAEA, (2008). "Thermophysical Properties of Materials for Nuclear Engineering: A Tutorial and Collection of Data", Vienna, Austria.
- [15] P.L. Kirillov, M.I. Terent'eva and N.B. Deniskina, (2007). "Thermophysical Properties of Nuclear Engineering Materials", third ed. revised and augmented, Izdat Publ. House, Moscow, Russia.
- [16] B. R. Frost, (1963). "The Carbides of Uranium", Journal of Nuclear Materials, Vol. 10, pp. 265-300.
- [17] D. Cox and A. Cronenberg, (1977). "A Theoretical Prediction of the Thermal Conductivity of Uranium Carbide Vapor", Journal of Nuclear Materials, Vol. 67, pp. 326-331.
- [18] L. B. Lundberg and R. R. Hobbins, (1992). "Nuclear Fuels for Very High Temperature Applications", Intersociety Energy Conversion Engineering Conference, San Diego, USA.
- [19] J. M. Leitnaker and T. G. Godfrey, (1967). "Thermodynamic Properties of Uranium Carbide", Journal of Nuclear Materials, Vol. 21, pp. 175-189.
- [20] J. A. Khan, T. W. Knight, S. B. Pakala, W. Jiang and R. Fang, (2010). "Enhanced Thermal Conductivity for LWR Fuel", Journal of Nuclear Technology, Vol. 169, pp. 61-72.

- [21] S. Ishimoto, M. Hirai, K. Ito, and Y. Korei, (1996). "Thermal Conductivity of UO<sub>2</sub>-BeO Pellet." *Journal of Nuclear Science and Technology*, Vol. 33, No. 2, pp.134-140.
- [22] R. Lattaa, S. T. Revankara, A. A. Solomona, (2008). "Modeling and Measurement of Thermal Properties of Ceramic Composite Fuel for Light Water Reactors". *Journal of Heat Transfer Engineering*, Vol. 29, No. 4, pp. 357-365.
- [23] McDeavitt, S. M. (2009). *High Conductivity Fuel Concept UO<sub>2</sub>-BeO Composite*. Retrieved Jan. 24, 2011, from [http://nuclear.tamu.edu/~ragusa/documents/courses/489\\_09C/lectures/NUEN\\_Ragusa\\_Guest\\_Lecture.pdf](http://nuclear.tamu.edu/~ragusa/documents/courses/489_09C/lectures/NUEN_Ragusa_Guest_Lecture.pdf).
- [24] Incropera, F. P., Dewitt, D. P., Bergman, T. L., and Lavine, A. S. (2006). *Fundamentals of Heat and Mass Transfer*, sixth ed. Wiley, USA.
- [25] Mokry, S., Gospodinov, Ye., Pioro, I. and Kirillov, P.L., (2009). *Supercritical Water Heat-Transfer Correlation for Vertical Bare Tubes*. Proc. ICONE-17, July 12-16, Brussels, Belgium, Paper #76010, 8 pages.
- [26] Zahlan, H., Groeneveld, D., and Tavoularis, S., (2010). *Look-Up Table for Trans-Critical Heat Transfer*. Proc. 2nd Canada-China Joint Workshop on Supercritical Water-Cooled Reactors (CCSC-2010), Toronto, Ontario, Canada: Canadian Nuclear Society, April 25-28.
- [27] K. Lassmann, and F. Hohlefeld, (1987). "The Revised Gap Model to Describe the Gap Conductance between Fuel and Cladding". *Journal of Nuclear Engineering and Design* 103, pp. 215-221.
- [28] B.J. Lewis, F.C. Iglesias, R.S. Dickson, and A. Williams. (2008). "Overview of High Temperature Fuel Behaviour". 10<sup>th</sup> CNS International Conference on CANDU Fuel., Ottawa, Canada, October 5-8.
- [29] P. Hu, and P. P. H. Wilson, (2010). "Supercritical Water Reactor Steady-State, Burnup, and Transient Analysis with Extended PARCS/RELAP5". *Journal of Nuclear Technology*, Vol. 172, pp.143-156.
- [30] K. M. Lee, M. Y. Ohn, H. S. Lim, J. H. Choi, S. T. Hwang, (1995). "Study on Models for Gap Conductance Between Fuel and sheath for CANDU Reactors". *Journal of Ann. Nucl. Energy*, Vol. 22, No. 9, pp. 601-610.
- [31] J. B. Ainscough, (1982). *Gap conductance in Zircaloy-Clad LWR Fuel Rods*. United Kingdom Atomic Energy Authority.